

# Relaxation phenomena in EDAMn<sub>1-x</sub>Cd<sub>x</sub>Cl<sub>4</sub> perovskite; 0 ≤ x ≤ 1 perovskite

M. A. AHMED

Physics Department, Faculty of Science, Cairo University, Giza, Egypt  
E-mail: moala47@hotmail.com

S. T. BISHAY

Physics Department, Faculty of Girls for Science, Art and Education Ain Shams University

M. A. GABAL

Chemistry Department, Faculty of Science, Benha University, Benha, Egypt

N. HELMY

Physics Department, Faculty of Girls for Science, Art and Education Ain Shams University

The electrical properties measurements were carried out for the complex (CH<sub>2</sub>)<sub>2</sub>Mn<sub>1-x</sub>Cd<sub>x</sub>Cl<sub>4</sub>, 0.0 ≤ x ≤ 1.0 at different temperatures as a function of frequency (100–1000 kHz). Four transition points were obtained for x = 0.5, which were assigned as thermochroism, interlayer exchange interaction, order-disorder and chain melting transition. The presence of more than one straight line in the conductivity data clarifies the presence of more than one conduction mechanism, and the calculated values of the activation energy indicate the semiconducting characteristics of the investigated complexes. The values of the relaxation time depend on Cd-content as well as the heating temperature. The expected critical concentration at x = 0.5 agrees well with the percolation theory of Mont-Carlo group. The IR spectra indicate that, the force constant of the bonds and the atomic mass vibration are affected by Cd-content.

© 2005 Springer Science + Business Media, Inc.

## 1. Introduction

There is wide range of applications in different technological fields specifying the diamine complexes where their type affects on the structure, thermal properties, particle size, morphologies, loading content, and release behavior of core materials of the microcapsules. Jeong *et al.* [1] showed that, ethylene diammine based polyurea microcapsules had a wider particle size distribution and much rougher surface as compared with the 1,6-hexane diamine based microcapsules. 1,6-Hexanediamine was also used to study the corrosion inhibition of mild steel in 1 M HCl at 60°C for 6 h. The percent inhibition was found to be in the range 40–93%. There is a dramatic increase in the percent inhibition by the synthesized materials as compared with the starting diamine [2]. While Joe *et al.* [3] studied the concept and synthetic strategies for the preparation of organic magnets using diamines. From the point of view of medical applications, diamines are used to elucidate the role of histamine in the pathogenesis of post-ischemic reperfusion injury of tissues. The effect of diamine oxidase (DAO) was studied on the changes in renal functions induced by 30 min occlusion followed by reperfusion of the renal vessels of unilaterally nephrectomized rats [4].

The diamine complexes [5–9] can be represented by the formula (CH<sub>2</sub>)<sub>m</sub>(NH<sub>3</sub>)<sub>2</sub>MX<sub>4</sub>, where m = 2, 3, 4, . . . . .; (NH<sub>3</sub>)<sub>2</sub> is the diamine group, M is the divalent transition metal ion (M = Cu<sup>2+</sup>, Ni<sup>2+</sup>, Mn<sup>2+</sup> . . .) and X is the halide ion (X = Cl<sup>-</sup>, Br<sup>-</sup>, I<sup>-</sup> and F<sup>-</sup>). The structure of these types of complexes can be represented as layers of two-dimensional MX<sub>4</sub><sup>2-</sup> tetrahedral or MX<sub>6</sub><sup>2-</sup> octahedral. The organic groups are sandwiched between and perpendicular to the metallic layers. The diamine groups lie in the hole under the metal ion, hydrogen bonded with the halide ion and covalently bonded with the hydrocarbon groups. The metal ions exist in the layers and arranged one up and one down, so that the line joining them form what is we called puckering effect. The spins are aligned antiferromagnetically within the layers and ferromagnetically ordered between the layers except in the case of Cu<sup>2+</sup> complexes, where the opposite alignment to takes place. The structure of the diamine complexes can be changed from symmetry to another depending on many factors such as: the ionic radius of the metal ion (M), the type of halide ions, the number of carbon atoms and the temperature.

El-Shaarawy *et al.* [10] studied the electric and magnetic properties of some organic complexes. The results

of the electrical properties showed some breaks, which can be attributed to dynamic disordering of organic chains. These results were correlated to the composition as well as the structure of the compounds. Ahmed *et al.* [11] studied the dielectric properties of some diamine complexes. They found that both  $\epsilon'$  and  $\epsilon''$  showed the same relaxation behavior which involve a large reorientable dipoles in the total polarization. The effect of metal ions on the dielectric properties of layered structure was studied by Abdel-Aal *et al.* [8] as a function of temperature and frequency.

The aim of this work includes the study of the variation of some electrical properties (dipole moment, ac-resistivity, activation energy, and relaxation time) for the  $(\text{CH}_2)_2\text{Mn}_{1-x}\text{Cd}_x\text{Cl}_4$ ,  $0.0 \leq x \leq 1.0$  with temperature (from 300 K up to near the melting point) at different frequencies between (100–1000 kHz). A correlation is made between the above mentioned properties to obtain the critical  $\text{Cd}^{2+}$  concentration. The IR-spectra is used to estimate the effect of the addition of  $\text{Cd}^{2+}$  ions on the complex structure in order to investigate the variation of stretched N–H on the expense of the bending N–H vibration.

## 2. Experimental

All chemical used in this work were of analar grade form (BDH). Stoichiometric ratios of  $(\text{CH}_2)_2(\text{NH}_3)_2\text{Cl}_2$  and  $\text{MnCl}_2 \cdot 4\text{H}_2\text{O}$  or  $\text{CdCl}_2 \cdot 5/2\text{H}_2\text{O}$  or both were dissolved in triply distilled water. The mixture was heated using water bath for two hours at  $70^\circ\text{C}$  until it reduced to one third of its initial volume. Plate like crystals were obtained during sudden cooling. Recrystallization was performed using distilled water. The final samples were washed using a mixture of ether and ethanol with ratio 2:1. The products then dried and grounded to a very fine powder and pressed into pellet form using a pressure of  $5 \times 10^8 \text{ N/m}^2$ . The two surfaces of each pellet are polished and covered with silver past (BDH) and checked for Ohmic conduction. The temperature of the sample was measured using Digi-Sense thermometer with K-type thermocouple, its junction in contact with the sample to prevent any temperature gradient. The accuracy of measuring temperature was better than  $\pm 1^\circ\text{C}$ . DSC thermographs were carried out for the samples in order to have information about the different structural properties. The electrical properties of the investigated samples were studied using bridge LCR Hi tester HIOKI model 353IZ (Japan). The accuracy of measuring the electrical properties was  $\pm 1\%$ . IR spectra were carried out for all complexes in the range from  $4000\text{--}1000 \text{ cm}^{-1}$  using Shimadzu IR-470 spectrophotometer to assure the formation of the main function groups.

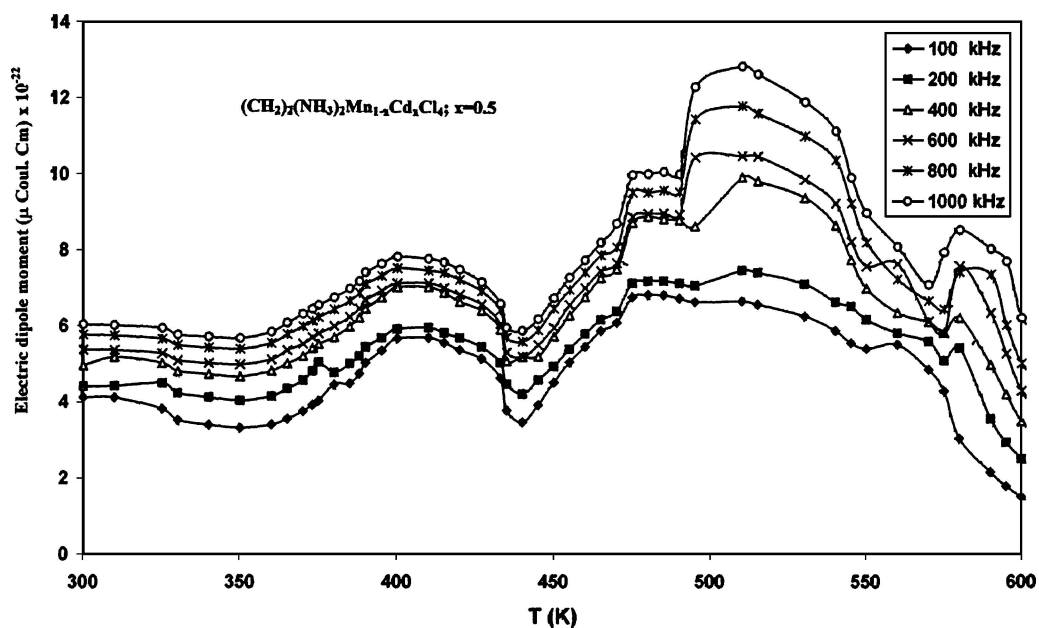
## 3. Results and discussions

Fig. 1a shows the variation of the electric dipole moment ( $\mu$ ) with absolute temperature ( $T$ ) for  $(\text{CH}_2)_2(\text{NH}_3)_2\text{Mn}_{1-x}\text{Cd}_x\text{Cl}_4$ ,  $x = 0.5$ , in the temperature range from 300 K up to near the melting point of

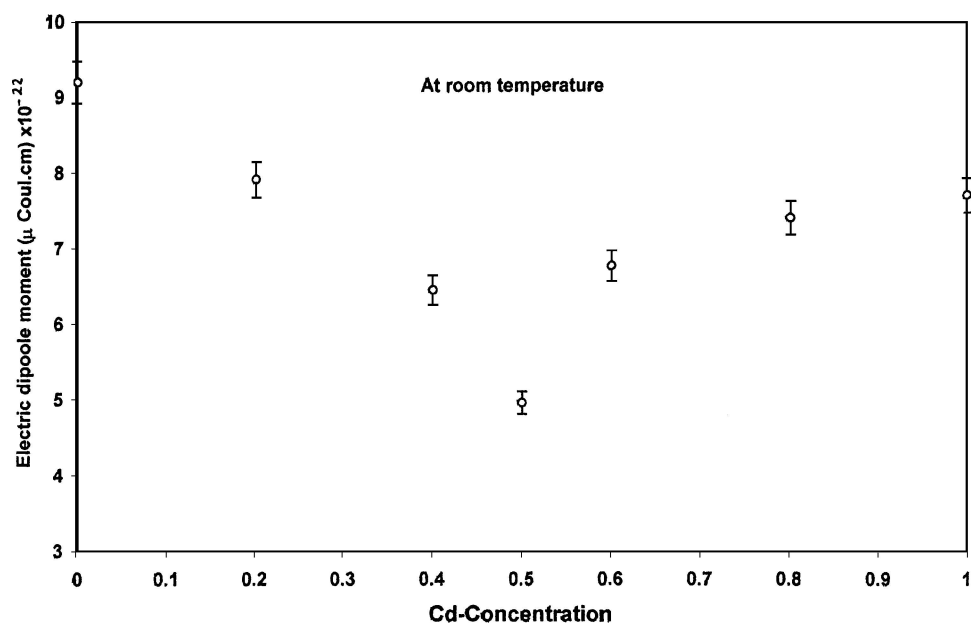
the sample, as a function of frequency (100–1000 kHz). The data shows that, the electric dipole moment is nearly temperature independent from room temperature up to about 360 K. This may be due to participation of some kinds of polarization such as electronic and atomic polarization [12]. It is known that [5, 13]: Some of the peaks obtained are accompanied by a change in the crystal symmetry, while others are accompanied by a transition from a complete crystalline order state to a complete disorder state. Above 360 K, it is noted that  $\mu$  increases with increasing temperature passing through four transition points at 405, 470, 510 and above 510 K. The positions of the first three transition temperatures are frequency independent, while the fourth varies its position depending on frequency. The first phase transition (405 K) is ascribed to thermochromism where a reversible color change is observed with temperature. This color depends on the metal; its oxidation states and its ligands. The thermochromic transition is also accompanied by a change in crystal symmetry. The second transition (470 K) is expected to be due to exchange interaction where the spacing between the planes plays a role in relaxing the polarized dipoles. At relatively high temperature, the system is changed from completely ordered state to completely disordered state giving rise to the third transition i.e., the thermal energy overcome the field effect of aligning the dipoles. Above 510 K, the large thermal energy increases the lattice vibration as well as the lattice scattering, consequently softening of some chemical bonds takes place giving rise to what is we called chain melting transition [14]. One of the peculiarities that appeared in Fig. 1a is the shift in the chain melting transition with increasing frequency toward the high temperature. This is because at high frequency the chain connecting the different dipoles has not sufficient time to be heated, which lag the chain melting. The polarization that takes place in this last region may be orientational polarization due to its temperature dependence [12].

Fig. 1b shows the variation of  $\mu$  with Cd-concentration at room temperature for frequency 400 kHz. The data show that, the values of  $\mu$  decrease with increasing  $x$  up to 0.5 and then increase. This may be due to the replacement of  $\text{Cd}^{2+}$  (ionic radius =  $0.94 \text{ \AA}$ ) by  $\text{Mn}^{2+}$  (ionic radius =  $0.74 \text{ \AA}$ ), which changes the canting angle as well as the puckering effect. While for  $x = 0.5$ , the uniform distributions of  $\text{Cd}^{2+}$  and  $\text{Mn}^{2+}$  ions form a symmetric shape. In other words, at this concentration the probability of the interlayer exchange interaction due to Cd-Cd and Mn-Mn dipoles is predominant, while for the others the predominant one is the Cd-Mn dipoles formation.

Fig. 2 is a typical curve illustrates the dependence of the ac conductivity ( $\ln\sigma$ ) on the reciprocal of absolute temperature ( $1000/T$ ) up to near the melting point of the sample in the frequency range from 100 to 1000 kHz for  $(\text{CH}_2)_2(\text{NH}_3)_2\text{Mn}_{1-x}\text{Cd}_x\text{Cl}_4$ ,  $x = 0.5$ . From the figure it is obvious that, the electrical conductivity increases with increasing temperature passing by four transition points corresponding to those appeared



(a)



(b)

Figure 1 (a) The change of electric dipole moment  $\mu$  with absolute temperature  $T(K)$  as a function of frequency (100 kHz– 1 MHz) for  $(CH_2)_2(NH_3)_2Mn_{1-x}Cd_xCl_4$ ;  $x=0.5$ . (b) The variation of the electric dipole moment  $\mu$  with Cd-concentration at room temperature at 400 kHz.

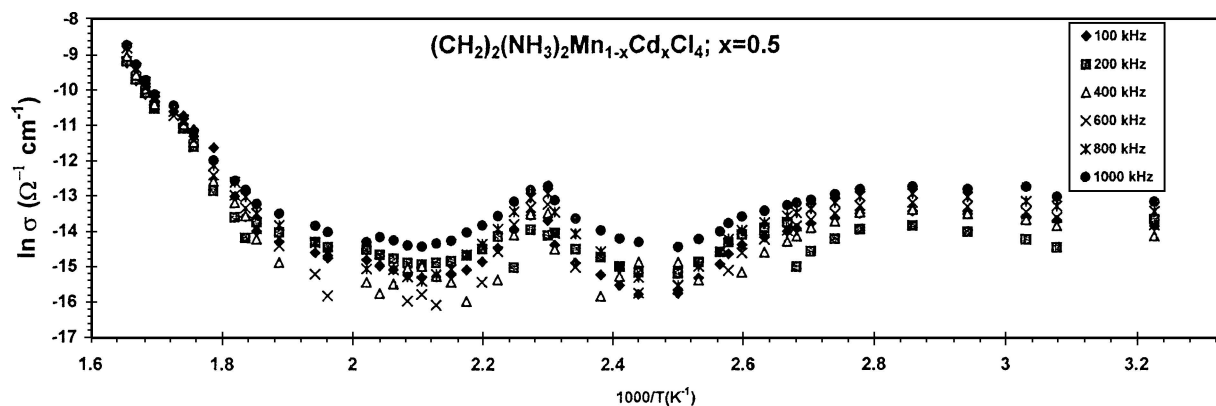
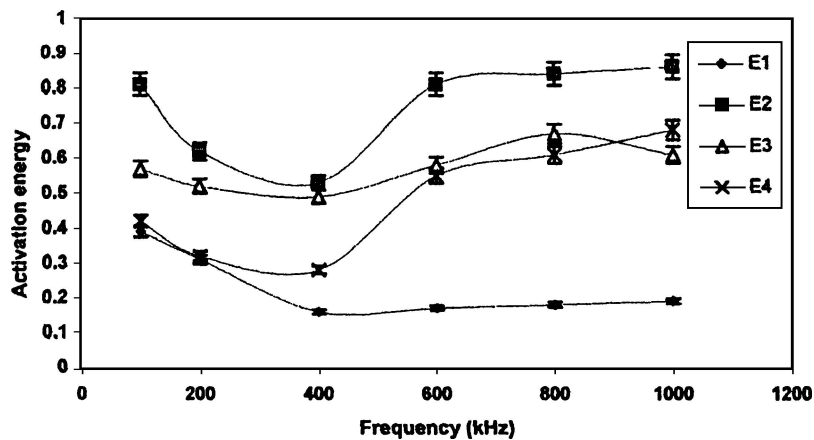
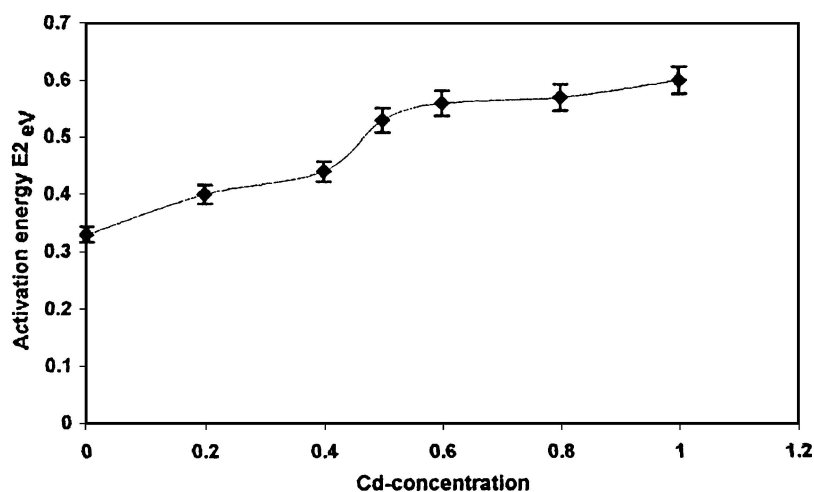


Figure 2 The dependence of the ac conductivity ( $\ln \sigma$ ) on the reciprocal of absolute temperature ( $1000/T$ ) in the frequency range (100–1000 kHz) for  $(CH_2)_2(NH_3)_2Mn_{1-x}Cd_xCl_4$ ;  $x=0.5$ .



(a)



(b)

Figure 3 (a) The dependence of the activation energy on the applied frequency for  $(\text{CH}_2)_2(\text{NH}_3)_2\text{Mn}_{1-x}\text{Cd}_x\text{Cl}_4$ ,  $x = 0.5$  in the four transition regions. (b) The dependence of the activation energy of the second transition region  $E_{II}$  on the Cd-concentration for the complexes  $(\text{CH}_2)_2(\text{NH}_3)_2\text{Mn}_{1-x}\text{Cd}_x\text{Cl}_4$ ,  $0.0 \leq x \leq 1.0$ .

in the temperature dependence of electric dipole moment relation Fig. 1a, where maximum value in  $\epsilon'$  identical to the minimum value of  $(\ln\sigma)$ , which is reasonable because  $\epsilon' \propto 1/\sqrt{\sigma}$  [15]. More than one straight line with different slopes is obtained in the relation of  $(1000/T, \ln\sigma)$  Fig. 2 clarifies the existence of different conduction mechanisms with different activation energies. All the obtained conductivity data obey the well known relation  $\sigma = \sigma_0 \exp(-E_a/kT)$ , where  $\sigma_0$  is the conductivity at absolute zero,  $k$  is the Boltzmann constant and  $E_a$  is the activation energy.

The dependence of the activation energy on the applied frequency for  $(\text{CH}_2)_2(\text{NH}_3)_2\text{Mn}_{1-x}\text{Cd}_x\text{Cl}_4$ ,  $x = 0.5$  in the four transition regions is shown in Fig. 3a. The data gives continues decrease in activation energy with increasing frequency up to 400 kHz, this means that, this is a critical frequency at which the value of the external frequency is equivalent to that of the oscillating ions (i.e., resonance frequency). At such frequency the pumping force effect is very large and more electrons will be transferred from one conduction state to another. The result of this process is the increase in the conductivity of the system this was enhanced by the minimum value of the activation energy obtained at 400 kHz. Fig. 3b shows the variation of the activation energy  $E_2$  with the Cd-concentration for

$(\text{CH}_2)_2(\text{NH}_3)_2\text{Mn}_{1-x}\text{Cd}_x\text{Cl}_4$ ,  $0.0 \leq x \leq 1.0$  at 400 kHz. The large values of the activation energy  $E_2$  enhance our expectation about the participation of ionic conduction mechanism in this region, where the conduction can be considered as partially electronic and partially ionic. The obtained data clarify that the samples under investigation can be regarded as semiconductor organic complexes. The data in Fig. 3b shows that the activation energy increases with increasing  $x$  up to about  $x = 0.5$  at which it reaches with shoulder nearly stable values. Though, the optimum conditions are obtained at this concentration ( $x = 0.5$ ), clarifying the critical behavior of  $\text{Cd}^{2+}$ . Above such concentration, the  $\text{Cd}^{2+}$  ions begin to represent the main skeleton with  $\text{Mn}^{2+}$  ion as a perturbation [7], vice versa after ( $x = 0.5$ ).

From the Cole-Cole data, the relaxation time  $\tau$  is calculated for  $(\text{CH}_2)_2(\text{NH}_3)_2\text{Mn}_{1-x}\text{Cd}_x\text{Cl}_4$ ,  $0.0 \leq x \leq 1.0$  at 300 and 500 K and reported in Table I, from which it is clear that, for all Cd-concentration  $\tau$  decreases with increasing temperature due to the diffusion of the charge carriers. Therefore, the time between electron phonon transitions decreases. From Table I, at the both temperature values,  $\tau$  decreases with increasing the Cd-content ( $x$ ) up to 0.5, after which  $\tau$  increases. This may be due to, the continuous replacement of  $\text{Cd}^{2+}$  instead of  $\text{Mn}^{2+}$  ions in the layer, which initiates a micro-strain

TABLE I The relaxation time  $\tau$  in  $\mu$  s for  $(\text{CH}_2)_2(\text{NH}_3)_2\text{Mn}_{1-x}\text{Cd}_x\text{Cl}_4$ ,  $0.0 \leq x \leq 1.0$  at 300 and 500 K according to the Cole-Cole

Complex	$\tau$ ( $\mu$ sec)	
	$T = 300$ K	$T = 500$ K
$(\text{CH}_2)_2(\text{NH}_3)_2\text{MnCl}_4$	4.59	2.25
$(\text{CH}_2)_2(\text{NH}_3)_2\text{Mn}_{0.8}\text{Cd}_{0.2}\text{Cl}_4$	4.56	2.16
$(\text{CH}_2)_2(\text{NH}_3)_2\text{Mn}_{0.6}\text{Cd}_{0.4}\text{Cl}_4$	2.12	1.16
$(\text{CH}_2)_2(\text{NH}_3)_2\text{Mn}_{0.5}\text{Cd}_{0.5}\text{Cl}_4$	1.23	0.87
$(\text{CH}_2)_2(\text{NH}_3)_2\text{Mn}_{0.4}\text{Cd}_{0.6}\text{Cl}_4$	6.97	1.21
$(\text{CH}_2)_2(\text{NH}_3)_2\text{Mn}_{0.2}\text{Cd}_{0.8}\text{Cl}_4$	12.11	4.11
$(\text{CH}_2)_2(\text{NH}_3)_2\text{CdCl}_4$	14.13	10.21

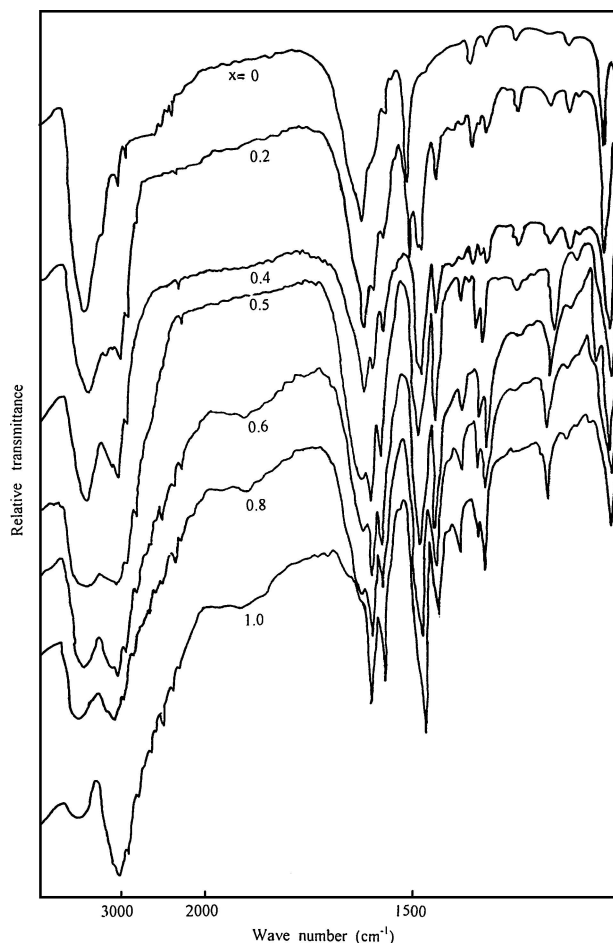


Figure 4 IR spectra for the complexes  $(\text{CH}_2)_2(\text{NH}_3)_2\text{Mn}_{1-x}\text{Cd}_x\text{Cl}_4$ ,  $0.0 \leq x \leq 1.0$ .

affecting directly on the conductivity as well as the relaxation time.

The percolation theory of Mont-Carlo group assigned that, the dilution of magnetic lattice by non-magnetic ions with complete 3d orbital, form a critical concentration at  $x=0.5$ . From the experimental data for the investigated samples, one find that a peculiarity was obtained in electric dipole moments, activation energy and the relaxation time at  $x = 0.5$  which agree well with the above mentioned theoretical work [5, 13].

The IR spectra is shown in Fig. 4 for  $(\text{CH}_2)_2(\text{NH}_3)_2\text{Mn}_{1-x}\text{Cd}_x\text{Cl}_4$ ;  $0.0 \leq x \leq 1.0$  were performed to assure the good preparation and to obtain an information about the crystal structure of the samples. The spectra exhibit regions of characteristic vibrations located at similar frequencies for all Cd-concentrations. The bands in the

region  $3000$  to  $3700$   $\text{cm}^{-1}$ , are assigned to stretching vibration (valence vibration) of di-ammonium group (N–H) bonds, which is appeared for the complex with  $x = 0$  as a sharp band and becomes broaden with increasing  $x$ . At about  $3000$   $\text{cm}^{-1}$  a small kink is observed its intensity as well as its peak width increase with increasing  $x$ . Peculiar behavior was obtained at  $x = 0.5$  where near about  $3300$   $\text{cm}^{-1}$  the intensity of two bands decrease and become shoulder like, which enhances our results about the critical behavior at such concentration. At lowest values of  $x$  the Mn-complex proportion forms the main skeleton while the Cd-complex proportion forms the perturbation and at  $x = 0.5$  the two proportions are equal. This behavior was observed from the graduation of the peak intensity and position in the considerable regions. The small band at  $2930$   $\text{cm}^{-1}$  is assigned to symmetric vibration of (C–H) in methylene group (–CH<sub>2</sub>–). The spectra show also that, by introducing cadmium in the complex an appearance of a new band at  $1590$   $\text{cm}^{-1}$  is observed, which is attributed to bending vibration of (N–H) bond. The intensity of this band is increased with increasing cadmium concentration, while the intensity of the other band characterizing the presence of manganese was decreased. This identifies the gradual replacement of manganese ion of small radius ( $0.74$  Å) by cadmium ion of larger radius ( $0.94$  Å), which affects drastically on the force constant and in turns the peak in the rang ( $1580$ – $1000$   $\text{cm}^{-1}$ ) will be varied in position and intensity. The observed shift in the band position due to the presence of Mn and Cd can be attributed to the effect of two factors: the bond force constant and the mass of vibrating atoms. The deformation vibration  $\delta_a(\text{NH}_3)$  can be observed around  $1580$   $\text{cm}^{-1}$ . This band is splinted by increasing Cd-content in the complex to appear as sharp band for  $x = 1.0$ . The sharp bands at  $1500$  and  $1020$   $\text{cm}^{-1}$  are assigned to bending vibration of (C–H) and (C–N) respectively. The other bands can be attributed to skeletal vibration.

#### 4. Conclusion

The thermochromic complexes are distinct by the existence of more than one phase transition. The investigated samples give four transitions shifted in position depending on the amount of the Cd-content and the applied frequency. The peculiarities obtained in the values of the activation energy, electric dipole moment and relaxation time at  $x = 0.5$  agree well with the expectation of the percolation theory as proposed by Scholl and Binder. The values of the activation energy are calculated from the experimental data indicate the semiconductor character of these complexes.

#### References

1. KI-JEONGHONG and SOO-MIN PARK, *J. Mat. Res. Bull.* **34**(6) (1999) 963.
2. SK. A. ALI and M. T. SAEED, *J. Polym.* **42**(7) (2001) 2785.
3. JOE. A. CRAYSTON, JOHN N. DEVINE and JOHN C. WALTON, *Tetrahedron Report no.* **541**(56) (2000) 7829.

4. H. KANEKO, S. KOSHI, T. HIRAOKA, Y. MIYAUCHI, N. KITAMURA and M. INOUE, *Biochimica et Biophys. Acta/Molecular Basis of Disease* **1407**(3) (1998) 193.
5. G. SORGE, H. MAAK and L. A. SHAVALOV, *Phys. Stat. Solidi (a)* **93** (1986) 315.
6. F. A. RADWAN, M. A. AHMED and H. MIKHAIL, *Solid State Commun.* **84** (1992) 1047.
7. K. A. DARWISH, M. MOUNIR, M. A. AHMED and G. H. ZAKI, *Thermochim. Acta* **255** (1995) 171.
8. M. M. ABD-EL-AAL and M. A. AHMED, *Physica B* **217** (1996) 133.
9. M. A. AHMED, S. M. ABDEL-WAHAB, A. M. IBRAHIM and F. A. RADWAN, *Assian J. Phys.* **7** (1998) 155.
10. M. G. EL-SHAARAWY, *J. Mag. Mag. Mater.* **217** (2000) 93.
11. M. A. AHMED, A. M. EL-REFAE, S. M. ABDEL WAHAB and F. A. RADWAN, *Indian J. Phys. (A)* **70** (1996) 593.
12. A. CHEKOWSKI, "Dielectric Physics" (Elsevier Scientific Publishing Company, Amsterdam, Oxford-New York, 1980).
13. M. A. AHMED, M. M. EL-DESOKY and F. A. RADWAN, *Aust. J. Phys.* **41** (1988) 85.
14. R. KEND, S. PLESKO, H. AREND, R. BLINE, H. ZEKS, J. SELINGER, B. LOZAV, J. SLAK, A. LEVSTIK and C. FILIPIC, *J. Chem. Phys.* **71** (1979) 2115.
15. C. G. KOOPS, *Phys. Rev.* **83** (1951) 121.

*Received 10 July 2003  
and accepted 22 July 2004*